

CRACK TIP FIELDS IN COARSE TWO PHASE MATERIALS
UNDER CREEP LOADING CONDITIONS

C. Broeckmann*, O. Lüsebrink*

A numerical study investigating the influence of ceramic hard phases in the cobalt base alloy CoCr26W5C1.2 on the crack tip parameters J and C^* is presented. A precracked plate under uniaxial tension (mode I) is modelled using the finite element method. The metal matrix is assumed to react elastic-viscoplastically, while the hard phases are assumed to behave linear elastically.

It is shown that J and C^* depend on the size, shape and distribution of hard phases ahead of the crack tip. The effect of local damage due to cleavage of a single hard phase is discussed.

INTRODUCTION

Wear resistant materials like ledeburitic chromium steels, high speed steels or cobalt base alloys consist of brittle ceramic carbides embedded in a metal matrix. On the one hand, an appropriate distribution of the coarse hard phases (HP) gives a significant rise in wear resistance (Franco (1)). On the other hand, this advantage is accompanied by a possible decrease in fracture toughness.

At room temperature, the effect of coarse ceramic particles on the behaviour of macroscopic cracks was examined in former work (Berns et al (2)). The fracture toughness depends on volume fraction, size and distribution of the HP as well as on the orientation of the global stress with respect to the material's axis of anisotropy. In many technical applications the material is exposed to mechanical loading under elevated temperatures. Time dependent material behaviour has to be taken into account. The topic of this paper is a numerical investigation of the influence of coarse HP on the parameters J and C^* describing the stress and strain fields ahead of a macroscopic crack in a two phase material with a metal matrix assumed to behave elastic-viscoplastically.

In the case of small scale yielding, the stress and strain fields ahead of a crack are

* Institute for Materials, Ruhr-University Bochum, Germany

determined by the stress intensity factor K . If plastic deformation is not neglectable, the J -integral concept becomes applicable. J is a contour integral calculated on paths enclosing the crack tip. As long as no unloading occurs, J is path independent. Assuming strain hardening according to the Ramberg-Osgood rule, the J -integral defines the intensity of the so-called HRR-fields describing local stress and strain ahead of a crack tip (Riedel (3)).

At elevated temperature the behaviour of most metal materials gets time dependent. The deformation is characterized by hardening processes in the early (primary) stage, followed by a period with a balance of hardening and softening (secondary or stationary 'creep' regime) and finally by a stage where increasing damage leads to rupture (tertiary 'creep' regime). Neglecting primary and tertiary creep, this behaviour can be described by a power law relationship between stress and strain rate (Norton's law) analogous to the relationship between stress and strain in the case of plastic deformation:

$$\dot{\epsilon}_{ij}^p = \frac{3}{2} \left\langle \frac{\sigma_{eq}}{K} \right\rangle^N \frac{s_{ij}}{\sigma_{eq}} \quad (1)$$

The analogy between the plastic and viscoplastic material laws leads to the definition of another integral C based on the formulation of J by replacing strain and displacements by their time derivatives (Landes and Begley (4)). This parameter determines the intensity of their HRR-fields for strain rate and stress in an elastic-viscoplastic material. In the early stage after loading, the elastic fields dominate over the plastic fields and the K -concept is still applicable. With time the creep zone grows and the C -integral, which is path and time dependent, has to be applied. With further plastic deformation the plastic zone spreads over a large part of the ligament and the deformation reaches a steady state. At this time, $C(t)$ no longer depends on path and time. The constant value of $C(t)$ is defined as C^* -integral (Fig. 1):

$$C^* = \int_{\Gamma} \left(U^* n_1 - \sigma_{ik} \frac{\delta \dot{u}_i}{\delta x_1} n_k \right) ds \quad (2)$$

The transition times between the validity of K , $C(t)$ and C^* may be obtained numerically (Broeckmann and Lüsebrink (5)).

NUMERICAL INVESTIGATIONS

The Numerical Model

The numerical studies were carried out with the FEM - program CRACKAN (Broeckmann (6)) assuming a geometrical linear theory and a state of plane stress. A single edge cracked plate was loaded under mode I conditions with a constant external stress $\sigma_N = 100$ MPa. The crack tip was modelled by a radius of $0.5 \mu\text{m}$ in order to restrict strains to a magnitude that can be handled by the applied theory. The influence of HP on the crack tip parameters was analysed by varying their arrangement in a refined mesh ahead of the crack tip (Figure 3).

The metal matrix was assumed to behave linear elastic viscoplastically. The stress is connected to the elastic strain by Hooke's law and the plastic strain rate is determined by

ECF 12 - FRACTURE FROM DEFECTS

eq. 1. Linear elastic behaviour is allocated to those elements of the FE-mesh representing HP. Table 1 shows the parameters corresponding to the cobalt base alloy CoCr26W5C1.2 with 12 vol% M_7C_3 -carbides tested at a temperature of $T = 800^\circ\text{C}$. Figure 2 displays the growth of the plastic zone, defined by lines of equal equivalent plastic strain, for the pure matrix material.

TABLE 1 - Material Parameters for the Numerical Simulation.

	E [MPa]	ν	K [MPa]	N
Matrix	130 000	0.3	9554	4.0
Hard Phases	300 000	0.3	-	-

Influence of a single Hard Phase

In a first study, the influence of a single HP on the crack tip parameters J and C^* was investigated. Figure 4a displays the results for a HP of constant size $h \times b = 40 \times 8 \mu\text{m}^2$, varying in distance d to the crack tip, figure 4b the results for a HP of the same size varying in its aspect ratio h/b . Each crack parameter is evaluated on paths surrounding the crack tip but not the HP. The plotted data are normalised by the results for the homogeneous matrix ($J_{\text{hom}}, C^*_{\text{hom}}$).

Influence of Hard Phase Distribution

In order to examine the influence of the distribution of hard phases on the crack tip parameters, different arrangements of HP were modelled. Figure 5 displays the different FE-meshes, with a HP volume fraction of 12%. Figure 6 shows the results for J and C^* , again normalised by the results for the homogeneous matrix.

Influence of Hard Phase Failure

It is well known that fracture mechanical parameters are affected by local damage ahead of a crack tip (2). In this study the influence of cleavage of a single HP ($d=13.6 \mu\text{m}$, $h \times b=40 \times 8 \mu\text{m}^2$, $h/b=5$) is investigated. A broken HP is modelled by introducing a microcrack within the particle prior to loading. Table 2 shows the results of this study.

TABLE 2 - Crack Tip Parameters: Path 1 runs between Crack Tip and HP, Path 2 surrounds the HP.

	Homogeneous Matrix	Hard Phase	Cleavage of Hard Phase
J [N/mm]	0.0233	0.0201	0.0217 (Path 1) 0.0226 (Path 2)
C^* [10^{-5} N/mm s]	0.1443	0.0838	0.0670 (Path 1) 0.1438 (Path 2)

DISCUSSION

For elastic-viscoplastic behaviour the crack tip loading is described by the stress intensity factor K in the early stage of loading, where plastic deformation is neglectable compared to

elastic deformation, and the parameter C^* in the later stage. The J-integral can replace K by the relationship $K = (E' \cdot J)^{0.5}$, with $E' = E$ (plane stress) and $E' = E/(1-\nu)^2$ (plane strain). This is done here for numerical reasons. Since J and C^* describe the crack tip loading, a decrease in J or C^* means an increase in crack resistance. Fig. 4 shows the influence of a single ceramic HP on both parameters. The nearer the distance of the HP to the crack tip, the lower is the value of J and C^* . A high aspect ratio, describing the elongation of the HP perpendicular to the crack, leads to low crack tip parameters. This influence is more pronounced for the parameter C^* than for J and K, respectively. The distribution of the HP depends on the manufacturing process. The banded models, representing the microstructure of a forged material, show the highest crack resistance in the L-T case. In the net-like model (representing the as cast state) the crack tip loading depends on the position of the crack tip with respect to the HP. If the whole cell lies ahead of the crack tip, the crack tip loading shows a minimum. If the crack tip lies within the cell, the loading increases with increasing distance to the HP-net. Again, the influence is more pronounced for the parameter C^* (Fig. 5, 6).

Cleavage of HP makes it necessary to assess the results more detailed: interpreting J and C^* as energy flow towards all defects within the integration path (Eshelby (7)), one has to distinguish between the main crack tip and the 2 tips of the microcrack at the broken HP. The overall flow towards both cracks (Table 2, Path 2) is higher compared to a configuration with an undamaged HP. The loading of the main crack, described in terms of J (short times), increases with failure of the HP, while in terms of C^* (longer times) the loading decreases (Table 2, Path 1). Experiments show that failure of HP occurs, if a critical normal stress is achieved within the HP. This indicates a negative influence of HP, if the critical normal stress is reached in an early stage, e.g. during loading of the structure. If HP-cleavage occurs in a later stage, i.e. when the whole structure is in a steady state and C^* is the correct parameter for the characterization of the crack tip fields, C^* can not be used as criterion for the onset of the growth of the main crack. Continuum damage models should be used instead.

CONCLUSIONS

Numerical studies were carried out showing the influence of coarse ceramic hard phases on the crack tip parameters under creep loading conditions. It was shown, that the parameters J and C^* are low for a high aspect ratio and a short distance of the hard phases to the crack tip. On the other hand, failure by cleavage of hard phases leads to an increase of the crack tip loading. Under stationary creep conditions this effect has to be examined using continuum damage models.

This work was supported by the Deutsche Forschungsgemeinschaft (DFG) within the project SFB316-TP G6.

SYMBOLS USED

C^* = C^* -integral (N/mm s)	U^* = rate of strain energy density (Mpa/s)
E = Young's Modulus (MPa)	\dot{u}_i = displacement rate (mm/s)
h/b = aspect ratio of hard phase	Γ = integration path
J = J-integral (N/mm)	$\dot{\epsilon}_{ij}^p$ = plastic strain rate (1/s)
K = material parameter (MPa)	σ_{eq} = von Mises effective stress (MPa)

ECF 12 - FRACTURE FROM DEFECTS

N = stress exponent	σ_{ij} = stress (MPa)
n_i = outward normal vector	σ_N = external stress (MPa)
s_{ij} = deviatoric part of stress (MPa)	ν = Poisson's ratio

REFERENCES

- (1) Franco, S., "Wechselwirkung zwischen Matrix und Hartphasen beim Warmverschleiß", Fortschr.-Ber. VDI, Reihe 5, Nr. 435, Düsseldorf, Germany, 1996.
- (2) Berns, H. and Broeckmann, C. and Weichert, D., Engineering Fracture Mechanics, Vol. 58, No. 4, 1997, pp. 311-325.
- (3) Riedel, H., "Fracture at High Temperature", Springer Verlag, Berlin, 1987.
- (4) Landes, J.D. and Begley, J.A., in: Mechanics of Crack Growth, ASTM STP 590, American Society for Testing and Materials, 1976, pp. 128-148.
- (5) Broeckmann, C. and Lüsebrink, O., Proc. DVM-Arbeitskreis Bruchvorgänge, Dresden, Germany, 1998, pp. 129-139.
- (6) Broeckmann, C., "Bruch karbidreicher Stähle - Experiment und FEM-Simulation unter Berücksichtigung des Gefüges", Fortschr.-Ber. VDI, Reihe 18, Nr. 169, Düsseldorf, Germany, 1995.
- (7) Eshelby, J.D., "Energy Relations and the Energy-Momentum Tensor in Continuum Mechanics", in: Inelastic Behaviour of Solids, publ. McGraw-Hill, New York, 1970.

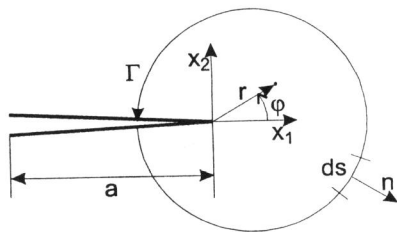


Figure 1 Integration path for J and C*

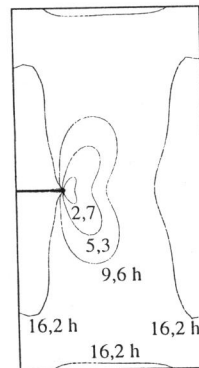


Figure 2 Evolution of plastic zone (lines of equal plastic strain)

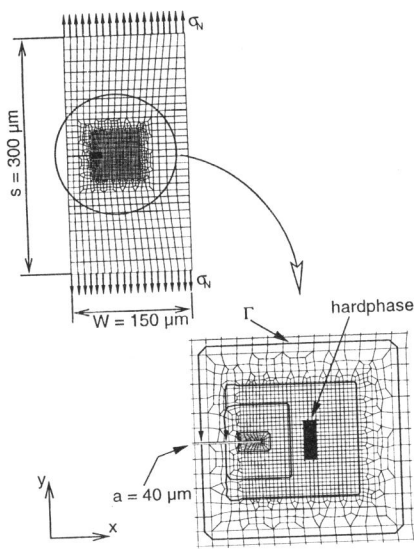


Figure 3 Single edge cracked plate under uniaxial tension (FE-model)

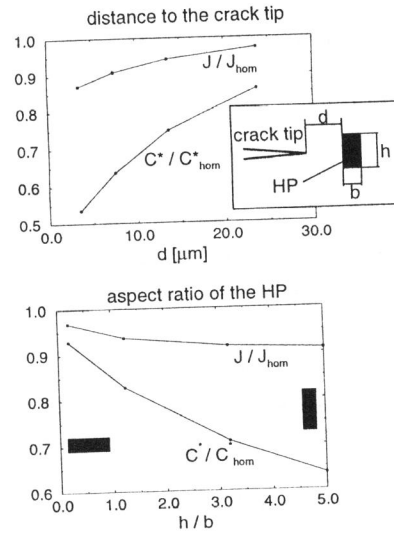


Figure 4 Influence of HP distance and aspect ratio on the parameter J and C^*

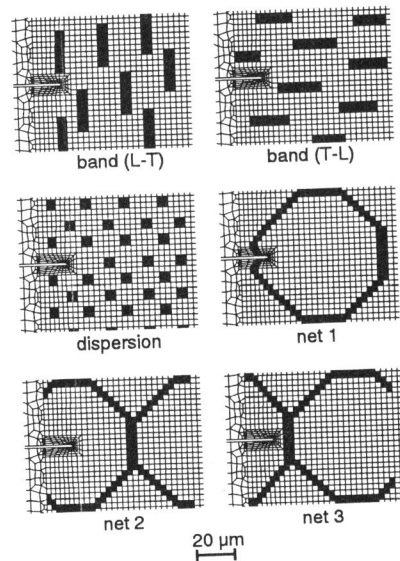


Figure 5 Distributions of HP (FE - meshes)

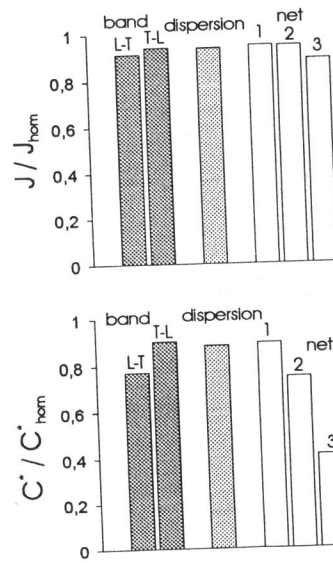


Figure 6 Influence of HP distribution on the parameters J and C^*